Achieving a high-Q response in metamaterials by manipulating the toroidal excitations

Yuancheng Fan,[1,*] Fuli Zhang,[1] Nian-Hai Shen,[2] Quanhong Fu,[1] Zeyong Wei,[3] Hongqiang Li,[3] and Costas M. Soukoulis[2,4]

[1]*Key Laboratory of Space Applied Physics and Chemistry, Ministry of Education and Department of Applied Physics, School of Science, Northwestern Polytechnical University, Xi'an 710129, China*

[2]*Ames Laboratory and Department of Physics and Astronomy, Iowa State University, Ames, Iowa 50011, United States*

[3]*Institute of Dongguan-Tongji University, Dongguan 523808, Guangdong, China*

[4]*Institute of Electronic Structure and Laser, FORTH, 71110 Heraklion, Crete, Greece*

(Received 20 December 2017; published 12 March 2018)

The excitation of toroidal multipoles in metamaterials is investigated for a high-Q response at a subwavelength scale. In this paper, we explore the optimization of toroidal excitations in a planar metamaterial comprised of asymmetric split ring resonators (ASRRs). It is found that the scattering power of a toroidal dipole can be remarkably strengthened by adjusting the characteristic parameter of ASRRs: an asymmetric factor. Interestingly, the improvement in toroidal excitation accompanies an increment of the Q factor of the toroidal metamaterial; it is shown that both the scattering power of the toroidal dipole and the Q factor increase more than one order by changing the asymmetric factor of ASRRs. The optimization in the excitation of a toroidal multipole provides an opportunity to further increase the Q factor of the metamaterial and boost light-matter interactions at the subwavelength scale for potential applications in low-power nonlinear processing and sensitive photonic applications.

DOI: 10.1103/PhysRevA.97.033816

I. INTRODUCTION

Optically resonant modes are of fundamental importance in realizing enhanced light-matter interactions for their coupling ability with light fields in both the spatial and time domain. For the spatial domain coupling, it is highly desirable to localize light in a possibly small volume for strong fields. Conventional dielectric microcavities have been reduced from the classical regime to the quantum regime where wave effects become dominant [1]. Plasmonic excitations in metallic structures have been exploited to realize light localization at deep subwavelength scales to join together with the well-developed nanoelectronic technology [2]. In contrast, for the time domain coupling, a dimensionless physical quantity, the quality factor (Q factor), is always adopted to measure energy damping relative to the stored energy of the oscillation, i.e., the photon lifetime of a resonant mode.

Metamaterials and metasurfaces [3–8], which allow light to interact with a medium in the resonant mode during its slow damping, are promising for the enhancement of light-matter interactions at a subwavelength scale. Various plasmonic metamaterials have been proposed to achieve a high-Q-factor response; for example, the trapped mode, which is weakly coupled to free space, was suggested to be excited by introducing symmetry breaking in the shape of structural elements to realize a sharp spectral response [9]. The trapped mode was later demonstrated in similar metamaterials and the resultant high-Q resonance [10,11] was utilized for applications in ultrasensitive spectroscopy and sensing [12], high-Q filtering [13,14], optical switching [15], nonlinear optics [16], and lasing spacers [17]. Recently, the excitation of a toroidal moment [18] in felicitously designed metamaterial was suggested as a solution for achieving a high-Q resonance [19,20]. The toroidal excitations are different from electrical and magnetic excitations in traditional multipole expansions [21,22]; it was found that the higher-Q response (in comparison to the original magnetic dipolar mode) in a metamaterial can be achieved by taking advantage of the weak free-space coupling of the toroidal dipolar excitation [23–25]. Later, the toroidal excitations were studied in oligomer nanocavities [26], coupled nanodisks [27–29], and coupled dielectric or metallic rods [30,31]. The exotic toroidal response was also investigated for optical manipulations in polarization control [32–35], high-Q subwavelength cavities [36–40], anapole excitation and/or invisibility [41–44], and optical force [45].

In this paper we propose achieving a higher-Q factor in a planar metamaterial by controlling the toroidal excitations. The unit cell, also called a metamolecule, of the metamaterial is comprised of four asymmetric split ring resonators (ASRRs). The magnetic resonance of the ASRRs can be excited by an electromagnetic wave with the polarization direction perpendicular to the gap of the ASRRs. The near-field coupling [23,46–49] of these magnetic resonators will induce a toroidal-moment-dominated fundamental resonance in the planar metamaterial. In the study we find that the excitation of the toroidal mode in a metamaterial can be significantly enhanced, while the Q factor of the planar metamaterial can be further improved through the control of toroidal excitations. Furthermore, the fundamental resonance is of a Fano line shape and the modulation depth of the resonance is nearly unity, which makes the toroidal metamaterials suitable for possible applications in ultrasensitive sensors. The toroidal geometry together with the Fano resonance gives rise to the high-Q response having enormous potential applications in low-threshold lasing, cavity quantum electrodynamics, and nonlinear processing.

*phyfan@nwpu.edu.cn

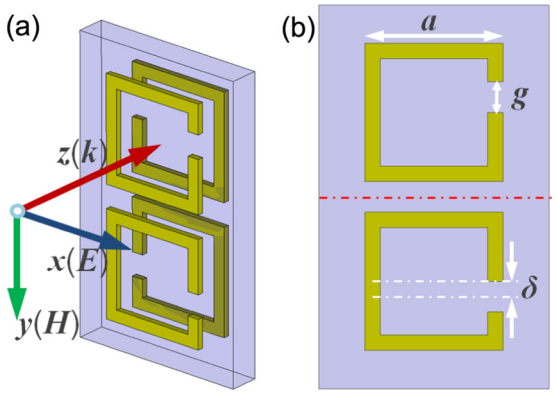

FIG. 1. (a) Schematic of a metamolecule of the toroidal metamaterial. The metamaterial is illustrated by a normal incident wave with the electric polarization along the x axis. (b) Top view of the metamolecule with the geometric size being labeled by white arrows and black letters.

II. RESULTS AND DISCUSSION

The metamolecule or the unit cell of the designed two-dimensional metamaterial is presented in Fig. 1. The rectangular unit cell is periodically translated along the x and y axes to form a planar toroidal metamaterial; the lattice constants along the x and y directions are 5 and 10 mm, respectively. As can be seen from the figure, the metamaterial is comprised of two patterned metallic layers and a dielectric spacer layer; the metallic layers are patterned into arrays of ASRRs. Four ASRRs are properly arranged to control the structural symmetry of the metamolecule: Pairs of ASRRs on the same layers are of mirror symmetry about the xz plane; pairs of ASRRs on different layers are of twofold rotational symmetry about the y axis. The distance between the ASRRs on the same layer in a metamolecule is set to 0.8 mm, which ensures that the ASRRs are closer to the ASRRs in the same unit cell (the ASSRRs are closer to the center [red dash-dotted line in Fig. 2(b)] of the metamolecule). The permittivity of the 0.8-mm-thick dielectric spacer is 2.55. The width of the metal strip is 0.5 mm and the outer width of the ASRRs is $a = 4$ mm. The asymmetry of the ASRRs was introduced in the square rings by opening gaps of size $g = 1$ mm positioned from the center (along the y direction) of the rings. An asymmetric parameter δ is defined as the lateral distance between the gap's center and the center of the ring [see Fig. 1(b)]. The asymmetric parameter introduces broken structural symmetry in the ASRRs and ensures the excitation of the magnetic dipolar mode; we will show that the undetermined asymmetric parameter is crucial in the control of the toroidal excitations. We performed all numerical calculations with a finite-difference-in-time-domain method [50] based electromagnetic solver [51]. We note that throughout our study the metamaterials are illuminated by x polarized (the electric field E is along the x axis) electromagnetic waves as illustrated in Fig. 1(a).

The ASRRs in the toroidal molecule are in close proximity; it is well known that the mutual interactions or couplings [52] between these building blocks play a determinative role in their collaborative response to incident fields. The couplings between the ASRRs in both the in-plane pair and the stacked

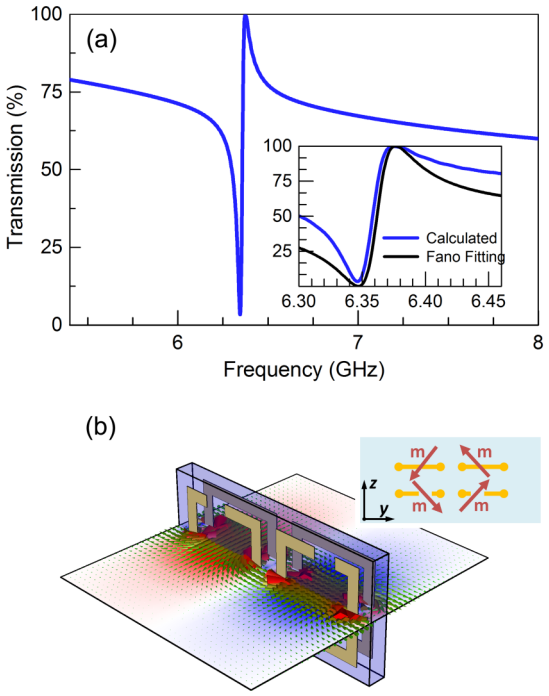

FIG. 2. (a) Calculated spectrum of a designed planar metamaterial with toroidal moment dominated Fano resonance. The asymmetric parameter was set equal to -0.4 mm. The inset shows a close-up of transmission near the resonant frequency. (b) Calculated spatial distributions of the vectorial magnetic field over the colormap of the z-component magnetic field on the central plane of a metamolecule at the peak frequency of the transmission spectrum. The inset illustrates the induced magnetic dipoles in the metamolecule forming a head-to-tail configuration of the toroidal dipole.

pair were studied in our previous work [36]. The in-plane ASRR pairs were designed with mirror symmetry with respect to the xz plane. The resonant frequency of the paired ASRRs is the same as that of ASRRs. Different from the metamaterials with period ASRRs, the mirror symmetry ensures that the paired ASRRs strongly couple to the incident waves, which means that the trapped magnetic mode of ASRRs can be well excited. To mimic the head-to-tail-shaped magnetic morphology of toroidal dipolar excitation in the bulk metamaterial, two layers of metallic ASRRs were stacked to couple the magnetic mode in ASRRs. The paired ASRRs on the top and lower layers in the metamolecule were designed to be of twofold rotational symmetry with respect to the y axis. This vertical coupling configuration provides a remarkable overlap between the magnetic dipoles of ASRRs on the top and lower layers, indicating strong magnetic coupling. The coupled magnetic modes in ASRRs show in-phase and out-of phase states at low and high frequencies, respectively. The high-frequency resonance is determined by the out-of-phase vertical coupling (not shown here). Since we mainly focus on the toroidal excitation in this paper, we show in Fig. 2 the transmission around the low-frequency resonance and the on-resonance local-field distribution; a close-up of the transmission near the resonant frequency is shown in the inset of Fig. 2(a).

The low-frequency resonance is determined by the in-phase vertical coupling [see the colormap of the z-component magnetic field in Fig. 2(b)] together with horizontal coupling under

normal electromagnetic incidence made by a circumfluent magnetic field or magnetic vortex, which is exactly the picture of toroidal dipolar [22,23] which shows a subwavelength electromagnetic localization within a dielectric substrate in a toroidal configuration. The underlying coupling mechanism in the planar toroidal metamaterial was investigated in Ref. [36]. The coupling of the induced magnetic dipoles in the metamolecule is illustrated in the inset of Fig. 2(b). The asymmetry of the ASRRs introduces the broken structural symmetry in the split ring resonators and ensures the excitation of magnetic dipoles [9,36]. The mirror symmetry of the metamolecule guarantees a symmetry-induced current distribution on the ASRRs on the same xy plane, which makes the in-plane magnetic dipoles oscillate with the opposite phase. Then the vertical coupling (coupling between ASRRs on different layers of twofold rotational symmetry) leads to an in-phase magnetic dipolar response around 6.4 GHz, a value we are concerned with in this study. These couplings of the induced magnetic dipoles leads to the dipoles being arranged in a head-to-tail configuration of the toroidal dipole.

To quantitatively evaluate the contributions to the electromagnetic scattering of the multipoles, we adopt the current density formalization [23] by integrating spatially distributed fields in a metamolecule. In the current density formalization, the radiating power of induced multipoles can be calculated with the formula

$$I = \frac{2\omega^4}{3c^3}|\boldsymbol{P}|^2 + \frac{2\omega^4}{3c^3}|\boldsymbol{M}|^2 + \frac{2\omega^6}{3c^5}|\boldsymbol{T}|^2 + \frac{\omega^6}{20c^5}M_{\alpha\beta}M_{\alpha\beta} + \cdots, \tag{1}$$

with the electric dipole moment

$$\boldsymbol{P} = \frac{1}{i\omega}\int \boldsymbol{j}\, d^3\boldsymbol{r}, \tag{2}$$

the magnetic dipole moment

$$\boldsymbol{M} = \frac{1}{2c}\int (\boldsymbol{r}\times\boldsymbol{j}) d^3\boldsymbol{r}, \tag{3}$$

the toroidal dipole moment

$$\boldsymbol{T} = \frac{1}{10c}\int [(\boldsymbol{r}\cdot\boldsymbol{j})\boldsymbol{r} + 2\boldsymbol{r}^2\boldsymbol{j}] d^3\boldsymbol{r}, \tag{4}$$

and the magnetic quadrupole moment

$$M_{\alpha\beta} = \frac{1}{3c}\int [(\boldsymbol{r}\times\boldsymbol{j})_\alpha \boldsymbol{r}_\beta + (\boldsymbol{r}\times\boldsymbol{j})_\beta \boldsymbol{r}_\alpha] d^3\boldsymbol{r}, \tag{5}$$

where $\boldsymbol{j}$ is the current density.

The radiating powers of the induced electric dipoles, magnetic dipoles, toroidal dipoles, and electric and magnetic quadrupoles were calculated in the simulation. We first study the radiating power of the multipoles for the metamaterial with the asymmetric parameter $\delta = -0.4$ mm (black dashed lines) (the minus sign means that the gap is away from the center of the metamolecule). For simplicity, we present in Fig. 3 the three mainly contributed multipoles of the metamaterials, including the electric dipole $\boldsymbol{P}_x$, toroidal dipole $\boldsymbol{T}_x$, and magnetic quadrupole M_{yz}. We note that the radiating powers of all other components of the multipoles are several orders lower in comparison with the three mainly contributed multipoles.

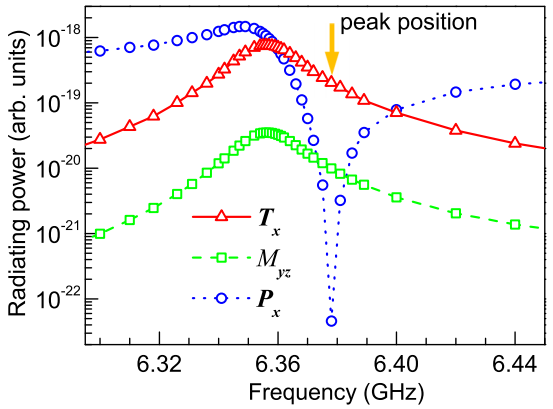

FIG. 3. Radiating power for induced multipoles of the planar toroidal metamaterial: the toroidal dipole (red solid curve), magnetic quadrupole (green dashed curve), and electric dipole (blue dotted curve).

The electric dipole $\boldsymbol{P}_x$ shows strong scattering in the whole frequency band, which reveals that the metamaterial is excited by the electric component of the incoming wave. The toroidal dipole $\boldsymbol{T}_x$ shows considerable scattering around the resonance; the x component of the toroidal dipole moment plays a dominant role at the transmission peak frequency of 6.38 GHz (marked with an arrow in Fig. 3) in comparison with other multipoles. The scattering of the magnetic quadrupole M_{yz} shows a similar frequency dependence on the toroidal dipole $\boldsymbol{T}_x$; however, the radiating intensity of the toroidal dipole $\boldsymbol{T}_x$ is 20 times bigger than that of the magnetic quadrupole M_{yz}. It is noteworthy that the magnetic quadrupole M_{yz} is the only component with a radiating contribution comparable to that of the toroidal dipole, which should be due to their similar coupling configurations of the magnetic dipoles on the yz plane.

The metamolecule of the toroidal metamaterial is constructed with ASRRs and the unusual property of the ASRRs is the high-Q trapped mode originating from the broken structural symmetry. The asymmetric parameter is crucial in the trap mode of ASRRs, which is the fundamental element in the formation of the toroidal mode. We thus investigated the influence of asymmetric parameters on the toroidal excitation in the metamaterial. Figure 4 shows that the scattering power of the induced electric dipole changes only slightly when the asymmetric parameter changes. In stark contrast, the scattering power of the toroidal dipole changes significantly with the change of the asymmetric parameter: The toroidal moment is stronger with small asymmetric parameters and when the gap is close to the center of toroidal metamolecule. The trap mode of the ASRR is sensitive to the asymmetric parameter: An ASRR with a small asymmetric factor is weakly coupled to external stimuli and shows stronger binding in the time domain; then the excited in-phase magnetic mode or toroidal mode becomes even stronger compared to the bigger asymmetric factor.

Intuitively, the improvement in exciting the toroidal dipole will be beneficial to achieving a higher-Q response in the metamaterials since both the higher Q with smaller asymmetry and the enhanced toroidal excitations are promising in binding electromagnetic waves. The Q factor of a symmetric Lorentzian resonance can be calculated from the ratio of the central frequency to the FWHM, which is quite convenient.

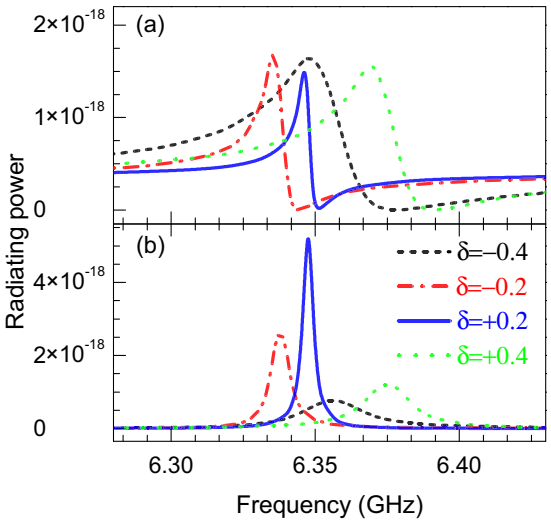

FIG. 4. Radiating power for induced multipoles of the planar toroidal metamaterial with different asymmetric parameter δ: (a) the electric dipole and (b) the toroidal dipole.

In the meanwhile, the Q factors of the asymmetric Fano resonance [53,54] have always been obtained by fitting the spectrum with a Fano formula

$$I \propto \frac{(F\gamma + \omega - \omega_0)^2}{(\omega - \omega_0)^2 + \gamma^2}, \tag{6}$$

where ω_0 and γ represent the position and width of the Fano resonance, respectively, and F is the Fano parameter [54]. There are two ways to define Q factors: (i) energy stored in the resonator or energy lost per cycle and (ii) resonant frequency or FWHM. Here we propose the extraction of the Q factor from characteristic frequencies (dip and peak frequencies f_d and f_p, respectively) of the Fano resonance, which can be understood as the counterpart to the latter in the Fano resonance. The Fano-shaped asymmetric resonance originates from interference between a sharp resonance (discrete state) and the continuum (background). The resonant region lies between the dip and peak frequencies and f_d and f_p correspond to the destructive and constructive interferences, respectively. The central frequency of the Fano resonance would be $(f_d + f_p)/2$ and the FWHM would be $|f_d - f_p|/2$; then the Q factor of a Fano resonance can be obtained in comparison with the Lorentzian resonance

$$Q = \frac{f_d + f_p}{|f_d - f_p|}. \tag{7}$$

Figure 5 plots the resonant frequencies (blue circles) and calculated Q factors (black spheres) of the toroidal metamaterials with different asymmetric parameter δ (changing from -0.4 mm to $+0.4$ mm). The calculated Q factors using Eq. (7) agree well with fitted results using the Fano formula (6). Taking the case in Fig. 2 ($\delta = -0.4$ mm) as an example, we plot in the inset of Fig. 2(a) the fitted spectrum using Eq. (6); the parameters were set as $F = 1$, $\omega_0/2\pi \approx 6.36$ GHz, and $\gamma/2\pi \approx 14.7$ MHz. The Q factor ω_0/γ is the same as the result calculated from Eq. (7). We can clearly see that the Q factor of the toroidal metamaterial increases significantly with small asymmetric parameters and when the gap is close

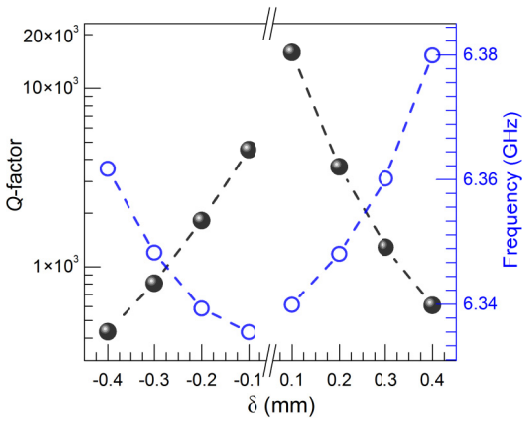

FIG. 5. Resonant frequencies (blue circles) and Q factors (black spheres) of the toroidal metamaterials with the asymmetric parameter δ changing from -0.4 mm to $+0.4$ mm.

to the center of toroidal metamolecule, the Q factor of the metamaterial increases to 15 849 ($\delta = 0.1$ mm) from 432 ($\delta = -0.4$ mm). It is noteworthy that the changes of the Q factor, resonant frequency, and radiating power are not in duality between negative and positive asymmetric parameters. This is due to the distance between the ASRRs on the same layer in a metamolecule being properly designed to achieve strong in-plane coupling as well as toroidal excitations in the metamolecule (see Fig. 1). The geometry of the unit cell ensures the coupling between ASRRs of different unit cells being stronger than the coupling between ASRRs in the same unit cell. Comparing the scattering of the toroidal dipole [in Fig. 4(b)] and the Q factor of the toroidal mode, we can find that the variation tendency of the Q factor is identical to the scattering power of toroidal excitations, which confirms the prediction that the Q factor of the toroidal metamaterial can be increased by optimizing the excitation of the toroidal dipole. Additional numerical studies confirm that the improvement in the Q factor through the optimization of the toroidal excitation is also valid in the case of a toroidal metamaterial with a realistic metal and commercial microwave substrate.

III. CONCLUSION

We have studied the toroidal excitation in a planar metamaterial comprised of ASRRs. We have shown that the toroidal excitation in a planar metamaterial can be controlled by tuning the asymmetric factor of ASRRs and the enhancement in toroidal excitation can remarkably improve the Q factor of the toroidal metamaterial. The high-Q feature of the toroidal metamaterial and the further improvement of high Q through geometric optimization may be beneficial to enhance light-matter interactions at a subwavelength scale for low-power nonlinear processing and sensitive photonic application.

ACKNOWLEDGMENTS

The authors would like to acknowledge financial support from the National Science Foundation of China (Grants No. 61505164, No. 61771402, No. 11372248, No. 11674266, No. 11674248, and No. 11404213) and the Fundamental Research

Funds for the Central Universities (Grant No. 3102017zy033). Work at Ames Laboratory was partially supported by the US Department of Energy, Office of Basic Energy Science, Division of Materials Science and Engineering (Ames Laboratory is operated for the US Department of Energy by Iowa State University under contract No. DE-AC02-07CH11358). Work at FORTH was supported by the European Research Council under the ERC Advanced Grant No. 320081 (PHOTOMETA).

[1] H. Cao and J. Wiersig, Rev. Mod. Phys. **87**, 61 (2015).
[2] E. Ozbay, Science **311**, 189 (2006).
[3] D. R. Smith, J. B. Pendry, and M. C. K. Wiltshire, Science **305**, 788 (2004).
[4] C. M. Soukoulis and M. Wegener, Nat. Photon. **5**, 523 (2011).
[5] N. I. Zheludev and Y. S. Kivshar, Nat. Mater. **11**, 917 (2012).
[6] A. V. Kildishev, A. Boltasseva, and V. M. Shalaev, Science **339**, 1232009 (2013).
[7] S. B. Glybovski, S. A. Tretyakov, P. A. Belov, Y. S. Kivshar, and C. R. Simovski, Phys. Rep. **634**, 1 (2016).
[8] Y. Fan, T. Qiao, F. Zhang, Q. Fu, J. Dong, B. Kong, and H. Li, Sci. Rep. **7**, 40441 (2017).
[9] V. A. Fedotov, M. Rose, S. L. Prosvirnin, N. Papasimakis, and N. I. Zheludev, Phys. Rev. Lett. **99**, 147401 (2007).
[10] I. A. I. Al-Naib, C. Jansen, and M. Koch, Appl. Phys. Lett. **94**, 153505 (2009).
[11] K. Aydin, I. M. Pryce, and H. A. Atwater, Opt. Express **18**, 13407 (2010).
[12] C. Wu, A. B. Khanikaev, R. Adato, N. Arju, A. A. Yanik, H. Altug, and G. Shvets, Nat. Mater. **11**, 69 (2012).
[13] O. Paul, R. Beigang, and M. Rahm, Opt. Express **17**, 18590 (2009).
[14] N. I. Zheludev, E. Plum, and V. A. Fedotov, Appl. Phys. Lett. **99**, 171915 (2011).
[15] M. Ren, B. Jia, J.-Y. Ou, E. Plum, J. Zhang, K. F. MacDonald, A. E. Nikolaenko, J. Xu, M. Gu, and N. I. Zheludev, Adv. Mater. **23**, 5540 (2011).
[16] V. R. Tuz, S. L. Prosvirnin, and L. A. Kochetova, Phys. Rev. B **82**, 233402 (2010).
[17] N. I. Zheludev, S. L. Prosvirnin, N. Papasimakis, and V. A. Fedotov, Nat. Photon. **2**, 351 (2008).
[18] V. M. Dubovik and V. V. Tugushev, Phys. Rep. **187**, 145 (1990).
[19] N. Papasimakis, V. A. Fedotov, V. Savinov, T. A. Raybould, and N. I. Zheludev, Nat. Mater. **15**, 263 (2016).
[20] Z. Liu, S. Du, A. Cui, Z. Li, Y. Fan, S. Chen, W. Li, J. Li, and C. Gu, Adv. Mater. **29**, 1606298 (2017).
[21] J. D. Jackson, *Classical Electrodynamics* (Wiley, New York, 1999).
[22] V. Savinov, V. A. Fedotov, and N. I. Zheludev, Phys. Rev. B **89**, 205112 (2014).
[23] T. Kaelberer, V. A. Fedotov, N. Papasimakis, D. P. Tsai, and N. I. Zheludev, Science **330**, 1510 (2010).
[24] Y.-W. Huang, W. T. Chen, P. C. Wu, V. Fedotov, V. Savinov, Y. Z. Ho, Y.-F. Chau, N. I. Zheludev, and D. P. Tsai, Opt. Express **20**, 1760 (2012).
[25] Z.-G. Dong, P. Ni, J. Zhu, X. Yin, and X. Zhang, Opt. Express **20**, 13065 (2012).
[26] B. Ögüt, N. Talebi, R. Vogelgesang, W. Sigle, and P. A. van Aken, Nano Lett. **12**, 5239 (2012).
[27] Z.-G. Dong, J. Zhu, X. Yin, J. Li, C. Lu, and X. Zhang, Phys. Rev. B **87**, 245429 (2013).
[28] Q. Zhang, J. J. Xiao, and S. L. Wang, J. Opt. Soc. Am. B **31**, 1103 (2014).
[29] C. Tang, J. Chen, Q. Wang, Z. Yan, B. Liu, F. Liu, and C. Sui, IEEE Photon. J. **8**, 4600209 (2016).
[30] A. A. Basharin, M. Kafesaki, E. N. Economou, C. M. Soukoulis, V. A. Fedotov, V. Savinov, and N. I. Zheludev, Phys. Rev. X **5**, 011036 (2015).
[31] H. Xiang, L. Ge, L. Liu, T. Jiang, Z. Q. Zhang, C. T. Chan, and D. Han, Phys. Rev. B **95**, 045403 (2017).
[32] N. Papasimakis, V. A. Fedotov, K. Marinov, and N. I. Zheludev, Phys. Rev. Lett. **103**, 093901 (2009).
[33] L.-Y. Guo, M.-H. Li, X.-J. Huang, and H.-L. Yang, Appl. Phys. Lett. **105**, 033507 (2014).
[34] Y. Bao, X. Zhu, and Z. Fang, Sci. Rep. **5**, 11793 (2015).
[35] T. A. Raybould, V. A. Fedotov, N. Papasimakis, I. Kuprov, I. J. Youngs, W. T. Chen, D. P. Tsai, and N. I. Zheludev, Phys. Rev. B **94**, 035119 (2016).
[36] Y. Fan, Z. Wei, H. Li, H. Chen, and C. M. Soukoulis, Phys. Rev. B **87**, 115417 (2013).
[37] C. Ding, L. Jiang, C. Sun, L. Wu, D. Xu, G. Zhang, and J. Yao, Phys. Status Solidi B **252**, 1388 (2015).
[38] S.-H. Kim, S. S. Oh, K.-J. Kim, J.-E. Kim, H. Y. Park, O. Hess, and C.-S. Kee, Phys. Rev. B **91**, 035116 (2015).
[39] H.-M. Li, S.-B. Liu, S.-Y. Liu, S.-Y. Wang, G.-W. Ding, H. Yang, Z.-Y. Yu, and H.-F. Zhang, Appl. Phys. Lett. **106**, 083511 (2015).
[40] M. Gupta, V. Savinov, N. Xu, L. Cong, G. Dayal, S. Wang, W. Zhang, N. I. Zheludev, and R. Singh, Adv. Mater. **28**, 8206 (2016).
[41] A. E. Miroshnichenko, A. B. Evlyukhin, Y. F. Yu, R. M. Bakker, A. Chipouline, A. I. Kuznetsov, B. Luk'yanchuk, B. N. Chichkov, and Y. S. Kivshar, Nat. Commun. **6**, 8069 (2015).
[42] W. Liu, J. Zhang, B. Lei, H. Hu, and A. E. Miroshnichenko, Opt. Lett. **40**, 2293 (2015).
[43] B. Luk'yanchuk, R. Paniagua-Domínguez, A. I. Kuznetsov, A. E. Miroshnichenko, and Y. S. Kivshar, Philos. Trans. R. Soc. A **375**, 20160069 (2017).
[44] A. A. Basharin, V. Chuguevsky, N. Volsky, M. Kafesaki, and E. N. Economou, Phys. Rev. B **95**, 035104 (2017).
[45] X.-L. Zhang, S. B. Wang, Z. Lin, H.-B. Sun, and C. T. Chan, Phys. Rev. A **92**, 043804 (2015).
[46] H. Xu, E. J. Bjerneld, M. Käll, and L. Börjesson, Phys. Rev. Lett. **83**, 4357 (1999).
[47] Y. Fan, J. Han, Z. Wei, C. Wu, Y. Cao, X. Yu, and H. Li, Appl. Phys. Lett. **98**, 151903 (2011).
[48] L. Cong, N. Xu, D. R. Chowdhury, M. Manjappa, C. Rockstuhl, W. Zhang, and R. Singh, Adv. Opt. Mater. **4**, 252 (2016).
[49] S. Yang, Z. Liu, X. Xia, Yiwen E, C. Tang, Y. Wang, J. Li, L. Wang, and C. Gu, Phys. Rev. B **93**, 235407 (2016).
[50] A. Taflove, *Computational Electrodynamics: The Finite Difference Time Domain Method* (Artech House, London, 1995).

[51] Z. Wei, Y. Cao, Z. Gong, X. Su, Y. Fan, C. Wu, J. Zhang, and H. Li, Phys. Rev. B **88**, 195123 (2013).

[52] Y. Fan, Z. Wei, J. Han, X. Liu, and H. Li, J. Phys. D **44**, 425303 (2011).

[53] S. Fan, Appl. Phys. Lett. **80**, 908 (2002).

[54] B. Luk'yanchuk, N. I. Zheludev, S. A. Maier, N. J. Halas, P. Nordlander, H. Giessen, and C. T. Chong, Nat. Mater. **9**, 707 (2010).